

# Testing of a 1.5-m Reflector Antenna at 322 GHz in a CATR Based on a Hologram

Janne Häkli, *Member, IEEE*, Tomi Koskinen, *Student Member, IEEE*, Anne Lönnqvist, Jussi Säily, Ville Viikari, *Student Member, IEEE*, Juha Mallat, Juha Ala-Laurinaho, Jussi Tuovinen, *Member, IEEE*, and Antti V. Räisänen, *Fellow, IEEE*

**Abstract**—Hologram-based compact antenna test range (CATR) is a potential method for testing large antennas at submillimeter wavelengths. This paper describes testing of a 1.5-m single offset parabolic reflector antenna with a 3-m-diameter hologram-based CATR. This is the first time such a measurement is carried out at submillimeter wavelengths. The antenna tests were done in a CATR that was specifically designed and constructed for these tests. The measured radiation pattern at the frequency of 322 GHz is presented. The measured pattern corresponds reasonably well to the simulated pattern of the antenna. The effect of the quiet-zone field nonidealities on the measurement results and the reasons for the discrepancies in the measured antenna beam are discussed.

**Index Terms**—Antenna measurements, compact antenna test range (CATR), hologram, submillimeter wave antennas.

## I. INTRODUCTION

**H**OLOGRAMS can be used as collimating elements in compact antenna test ranges (CATRs) [1], [2]. As a transmission-type device, a hologram is more economical to manufacture than large reflectors at submillimeter wavelengths due to less stringent surface accuracy requirements. The low costs also allow the design of a test-specific test range that can be built at the test site.

A hologram is a binarized interference pattern of an incident spherical wave and a plane wave. When it is illuminated with the spherical wave, the plane wave is radiated into the quiet zone of the CATR. The hologram pattern is designed iteratively with a computer by using finite-difference time-domain (FDTD) and physical optics (PO) based analysis of the hologram radiation [1]. The hologram pattern is manufactured by etching the binarized interference pattern on a copper-plated Mylar film. The pattern consists of curved slots that are less than  $\lambda/2$  wide. To reduce edge diffraction, the slots in the hologram pattern are narrowed toward the hologram edges to introduce amplitude taper to the hologram aperture field. The film is tensioned in a frame to

Manuscript received October 5, 2004; revised April 15, 2005. This work was supported in part by ESA/ESTEC under Contract 13096/98/NL/SB and in part by the Academy of Finland and Tekes under the Centre of Excellence program.

J. Häkli, T. Koskinen, A. Lönnqvist, J. Mallat, J. Ala-Laurinaho, V. Viikari, and A. V. Räisänen are with MilliLab, Radio Laboratory, Helsinki University of Technology, Espoo, FI-02015 TKK, Finland (e-mail: janne.hakli@tkk.fi).

J. Säily was with MilliLab, Radio Laboratory, Helsinki University of Technology, Espoo, FI-02015 TKK, Finland. He is now with VTT Information Technology, Espoo, FI-02044 VTT, Finland.

J. Tuovinen is with MilliLab, VTT Information Technology, Espoo, FI-2044 VTT, Finland.

Digital Object Identifier 10.1109/TAP.2005.856343

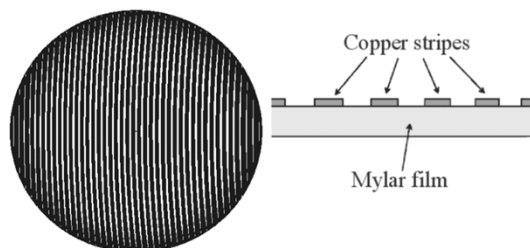


Fig. 1. An example of a hologram pattern. Copper stripes are shown in black and slots between them in white.

achieve sufficient surface flatness. Large holograms are etched in several pieces that are soldered together to form the complete hologram pattern [2]. An example of a hologram pattern is shown in Fig. 1.

Previously, a CATR based on a hologram has been used to test the Odin telescope antenna at the frequency of 119 GHz [3]. In this paper, the test results of a 1.5-m parabolic antenna obtained in a hologram-based CATR at the frequency of 322 GHz are presented. The CATR was designed and constructed specifically for this antenna test. The measured radiation pattern is compared to the simulated pattern of the antenna, and the effect of the quiet-zone field quality on the measurement results and the reason for the observed beam distortions are discussed.

## II. COMPACT ANTENNA TEST RANGE

### A. The Hologram and the Range Setup

The CATR used in the tests is based on a 3-m-diameter hologram, which consists of three separately etched pieces that were soldered together. The hologram manufacturing and range construction is described in detail in [2] and [4]. The CATR was built into the high voltage test hall at the Helsinki University of Technology and disassembled after the antenna tests two months later. Absorber walls were built to cover the walls of the hall and to block direct radiation from the hologram feed to the antenna under test (AUT). The schematic of the hologram CATR layout is presented in Fig. 2 and a photograph of the range is shown in Fig. 3.

The plane wave propagates in the direction of  $33^\circ$  in relation to the hologram normal. This tilt angle is used to avoid disturbances in the quiet-zone field caused by diffraction modes that propagate in the direction of the hologram normal. The field was measured with a network analyzer using a corrugated horn to probe the field. The probing was done using a plane polar scanner, which allowed the measurement of radial cuts of the quiet zone [2]. The

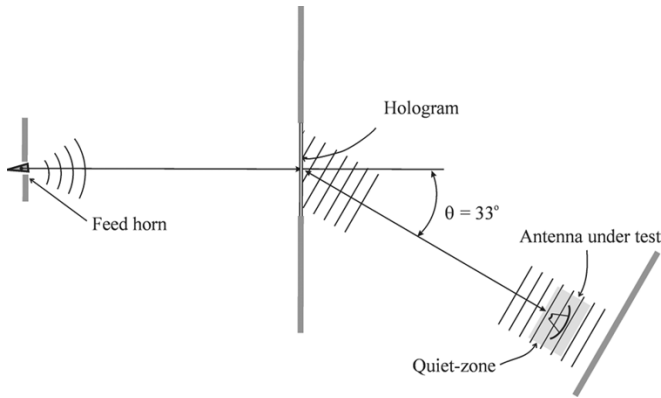


Fig. 2. The schematic of the CATR based on a hologram.

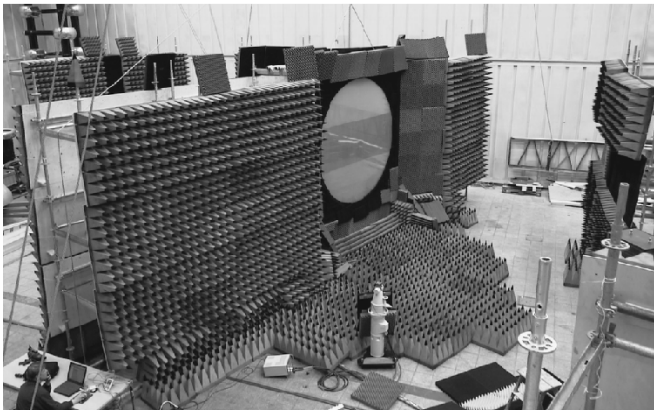


Fig. 3. Photograph of the CATR. The feed is located in the top left corner, the hologram is seen in the middle, and the AUT is placed in the bottom right corner.

measured amplitude and phase in horizontal and vertical cuts of the quiet-zone field are presented in Figs. 4 and 5.

The quiet-zone diameter was designed to be about 1900 mm, and measured maximum peak-to-peak deviation from a plane wave within the 1.5-m aperture of the antenna under test was about 2.6 dB in amplitude and  $250^\circ$  in phase at a frequency of 322 GHz. The typical peak-to-peak ripple was approximately 1 dB and  $10^\circ$  for the amplitude and for the phase, respectively. The quiet-zone phase front was saddle-shaped with concave phase front curvature in the vertical crosscut and convex phase front curvature in the horizontal crosscut. The main deformation in the measured amplitude was a dip in the middle of the quiet zone. The causes for the deviations from the plane wave are discussed in [2].

### B. Range Instrumentation

The transmitter and the receiver were supplied by EADS Astrium, Germany, and they are described in [5]. A corrugated horn was used as the feed to illuminate the hologram. The received power of the AUT was measured with a spectrum analyzer. The achieved dynamic range in the radiation pattern measurements was about 85 dB at 322 GHz.

The antenna positioner was built from a 40-mm Bofors anti-aircraft gun by the Laboratory of Machine Design of the Helsinki University of Technology, Finland. The original azimuth gear and the pedestal were conserved. A cradle-type elevation positioner was constructed from steel profile, and new azimuth and elevation drives were installed. Twenty-six-bit

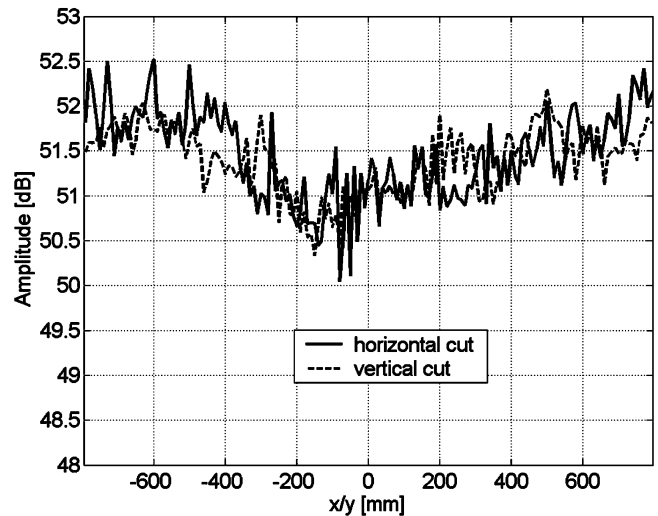


Fig. 4. Measured amplitude in the horizontal and vertical cuts of the quiet zone at 322 GHz.

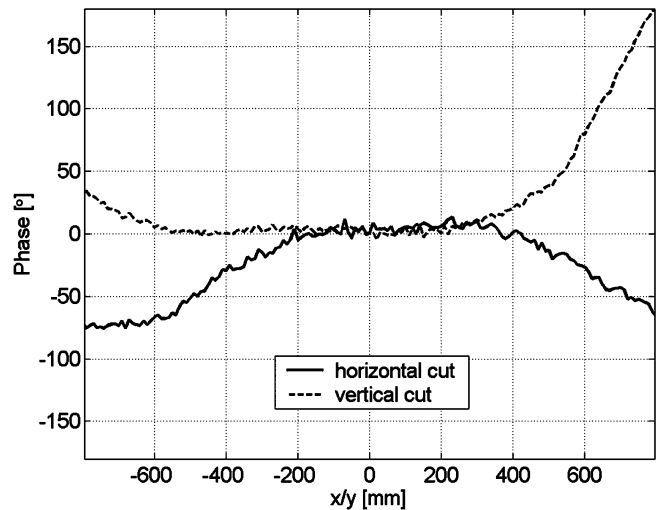


Fig. 5. Measured phase in the horizontal and vertical cuts of the quiet zone at 322 GHz.

absolute angle encoders were installed directly on the axes of rotation. The angle encoders are capable of measuring angular steps of 0.1 millidegrees. The antenna positioner and the measurement equipment were controlled with a PC using LabVIEW-based software that was developed for this purpose.

### III. MEASUREMENT RESULTS

The antenna under test was ADMIRALS representative test object (RTO), which was built by EADS Astrium, Germany, to demonstrate satellite antenna technology and to compare potential antenna testing methods at submillimeter wavelengths. The ADMIRALS RTO has a 1.5-m-diameter single offset fed paraboloid reflector with the focal length of 3 m. The feed offset angle is  $19.6^\circ$ . Previously, the RTO has been tested at 203, 322, and 503 GHz at EADS Astrium, and the 503 GHz results are presented in [6]. The antenna mounted on the antenna positioner is shown in Fig. 6.

The radiation pattern of the ADMIRALS RTO was measured at a frequency of 322 GHz at the linear vertical polarization.

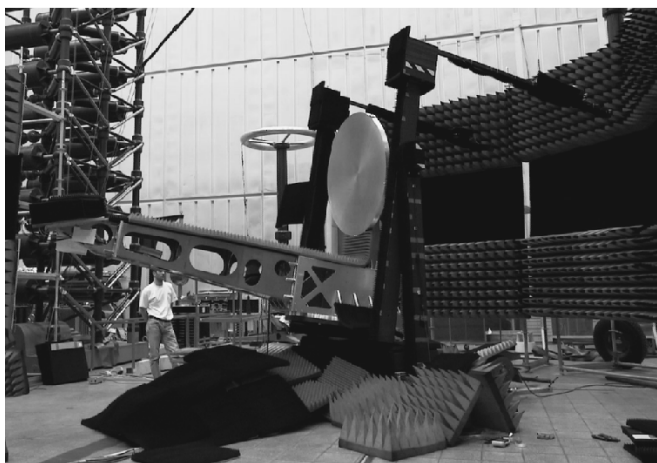


Fig. 6. Antenna under test (ADMIRALS RTO) on the antenna positioner.

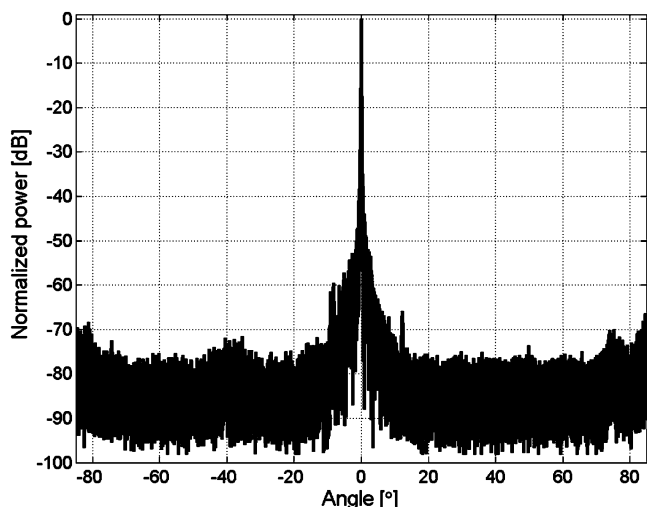


Fig. 7. Measured pattern cut in the  $H$ -plane (horizontal) at 322 GHz at the linear vertical polarization.

The pattern was measured in two cuts: in the  $E$ -plane (vertical) from  $-12^\circ$  to  $+12^\circ$  and in the  $H$ -plane (horizontal) from  $-85^\circ$  to  $+85^\circ$ . The direction of the maximum power in the radiation pattern was set as the origin of the antenna coordinate system. The measured  $H$ -plane pattern cut between  $\pm 85^\circ$  is shown in Fig. 7 and a closeup of the region between  $\pm 12^\circ$  is presented in Fig. 8. The  $E$ -plane pattern cut between  $\pm 12^\circ$  is shown in Fig. 9. A contour plot of the measured antenna radiation pattern is presented in Fig. 10. In all the figures, the measured power is normalized to 0 dB at the maximum.

The received power at the horizontal linear polarization was measured by switching the polarization of the receiver. The measured cross-polarization level in the  $H$ -plane cut is shown in Fig. 11 and the  $E$ -plane cut in Fig. 12.

The measured cross-polarization peak is approximately 22 dB below the peak at the copolarization (vertical polarization). The cross-polarization level is affected by the cross-polarization level of the quiet-zone field. Typical maximum cross-polarization level in a hologram based CATR is about  $-20$  dB [7].

The radiation of the antenna was simulated with the commercial reflector antenna software GRASP8W. The shape of the 1.5-m reflector surface was measured before the antenna was

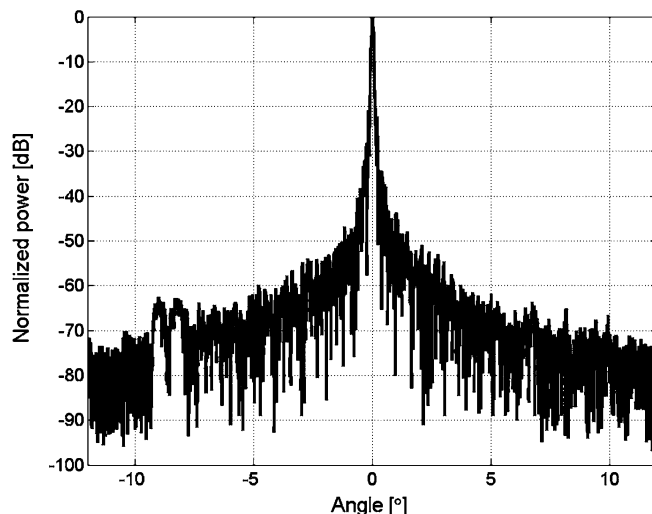


Fig. 8. Closeup of the measured  $H$ -plane cut at 322 GHz.

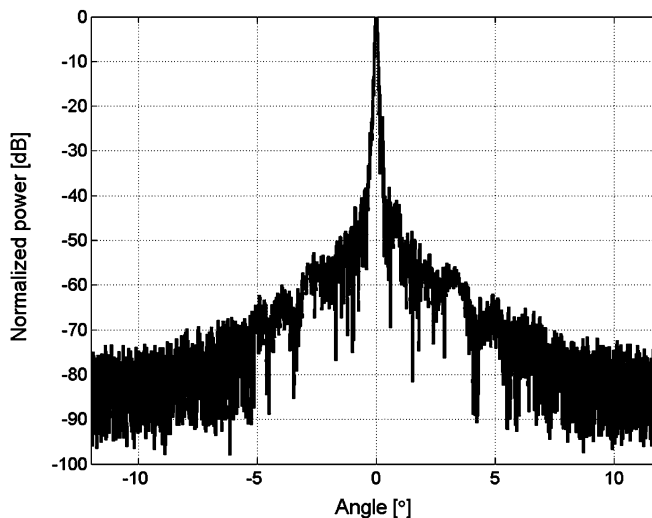


Fig. 9. Measured  $E$ -plane (vertical) cut of the antenna radiation pattern at 322 GHz.

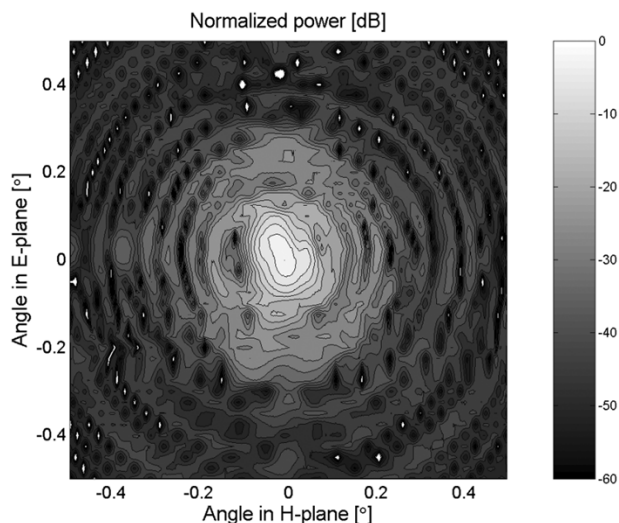


Fig. 10. Contour plot of the measured radiation pattern at 322 GHz. The contour interval is 3 dB.

assembled, and the effect of the reflector bending on the surface shape when it was attached to the antenna structure was

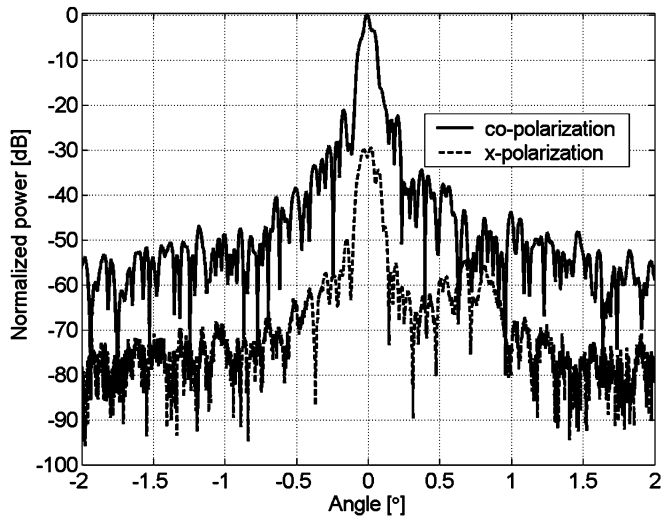


Fig. 11. Measured  $H$ -plane cut of the co- and cross-polarization pattern. The power is normalized to the maximum of the copolarized power.

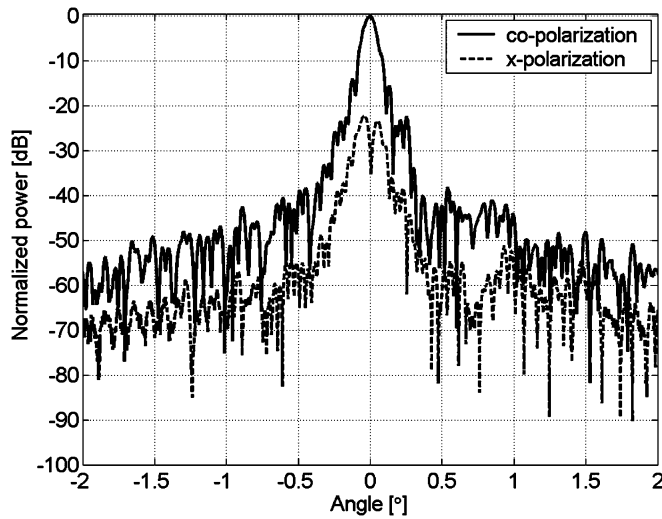


Fig. 12. Measured  $E$ -plane cut of the co- and cross-polarization pattern. The power is normalized to the maximum of the copolarized power.

estimated at EADS Astrium, Germany. These surface data were used to model the reflector in the simulations. A simple feed model with a Gaussian beam with a  $-10.5$  dB taper at an angle of  $13.5^\circ$  was used to illuminate the reflector. The focal length of the antenna was 3 m and the antenna was fed from the focal point of the paraboloid antenna. The radiation pattern was computed using PO and physical theory of diffraction (PTD). The  $H$ - and  $E$ -plane cuts of the simulated radiation pattern are presented in Figs. 13 and 14 together with the measured results.

The measured  $-3$  dB beam width is  $0.086^\circ$  in the  $E$ -plane and  $0.050^\circ$  in the  $H$ -plane. The corresponding simulated beam widths are  $0.053^\circ$  and  $0.045^\circ$ , respectively.

#### IV. EVALUATION OF THE RESULTS

The measured radiation pattern of the AUT is affected by the quality of the quiet-zone field and by deviations of the antenna structure from the designed structure. These factors affecting the measured antenna pattern are discussed next.

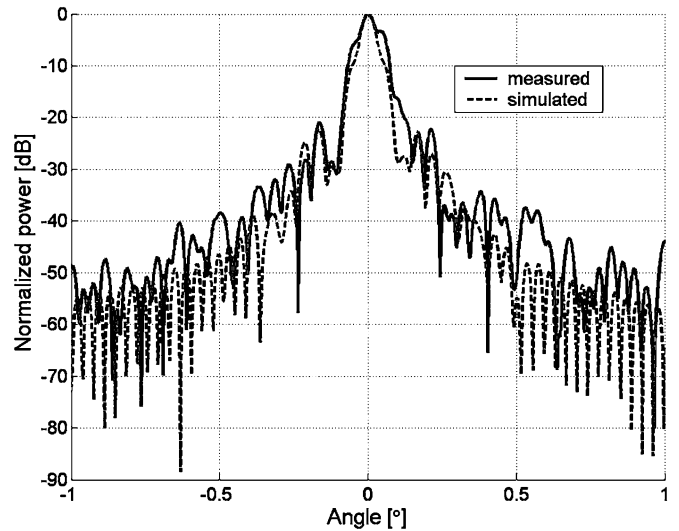


Fig. 13. Measured and simulated  $H$ -plane cuts of the radiation pattern at 322 GHz.

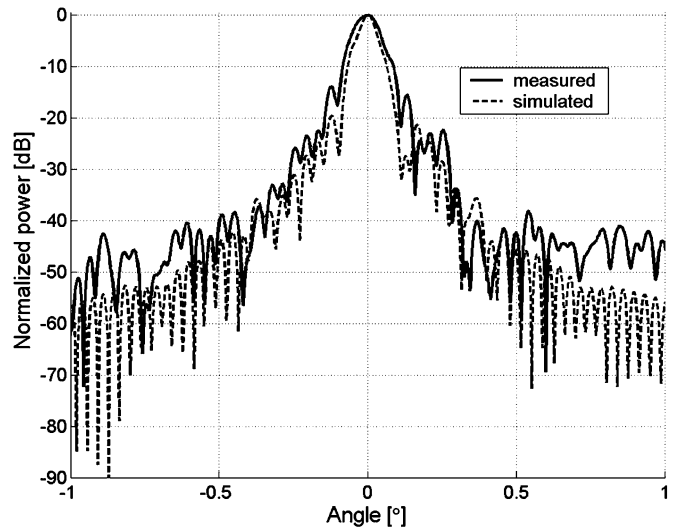


Fig. 14. Measured and simulated  $E$ -plane cuts of the radiation pattern at 322 GHz.

##### A. Effect of the Quiet-Zone Field Quality

The objective of the antenna testing is to determine the characteristics of the antenna, i.e., the actual radiation pattern of the antenna without any distortions due to external factors. Usually the high quality of the quiet-zone field ensures that the measured radiation pattern corresponds with good accuracy to the actual radiation pattern of the AUT. At submillimeter waves, it is very challenging to achieve a good quality quiet zone in a CATR, and the effect of the quiet-zone quality has to be taken into account in the evaluation of the measurement results.

The quiet-zone field deviations can be divided to systematic distortions, such as taper, and to ripple. The ripple is caused by scattering in the measurement range and by operation of the collimating element (surface or pattern errors in the hologram) and causes extraneous lobes in the measured radiation pattern when the main lobe is pointing toward the scatterer. The systematic distortions in the quiet-zone field are caused by the nonideal operation of the collimating element.

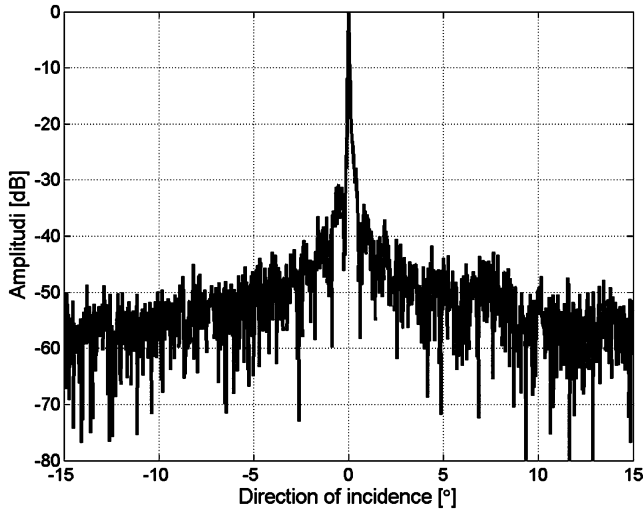


Fig. 15. Normalized angular spectrum of the quiet-zone field in the horizontal plane [2].

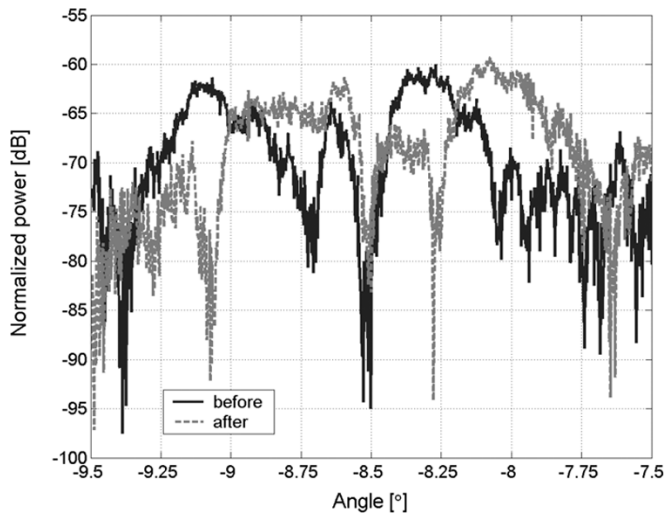


Fig. 16. Closeup of a measured side-lobe before and after the steering of the quiet-zone plane wave direction by  $0.22^\circ$ .

1) *Effects of the Quiet-Zone Ripple:* The quiet-zone field amplitude and phase were measured prior to the antenna tests (shown in Figs. 4 and 5), and the angular spectrum (plane wave spectrum) was computed to identify potential scatterers in the range. The angular spectrum of the quiet-zone field in the horizontal plane of the AUT is shown in Fig. 15.

The angular spectrum suggests that a possible disturbance (a so-called stray or spurious signal) to the quiet zone may originate around the direction of  $+8^\circ$  in the horizontal plane in relation to the antenna positioner [2]. This was verified by steering the plane wave direction by about  $0.22^\circ$  by moving the feed horn of the CATR. The locations of the scatterers in the hall remain the same, but the direction of the AUT main beam in relation to the antenna positioner changes by the amount of plane wave steering. We observed that the side-lobe around  $-8^\circ$  in the  $H$ -plane was relocated in the antenna coordinates by the amount of the plane wave steering and remained in the same direction in relation to the antenna positioner. This indicates that the measured side-lobe originates from the CATR instead of the antenna itself. Fig. 16 shows the side-lobe before and after the

plane wave steering. The origin of the antenna coordinates is at the main peak of the radiation pattern in both measurements.

The disturbance in the direction of  $+8^\circ$  in relation to the antenna positioner in the horizontal plane appears to originate inside the hologram aperture. This indicates that either scattering from the measurement environment on the AUT side of the hologram is reflected from the hologram surface or the main beam of the antenna receives through the semitransparent hologram reflections from the feed side of the hologram CATR (see CATR layout in Figs. 2 and 3). Inexpensive microwave absorbers that are not intended for submillimeter wavelengths were used to cover some of the walls at the feed side of the hologram CATR [2]. These absorbers are a potential source of reflections in the hall.

The effects of the spurious signals on the measured radiation pattern can be compensated using antenna pattern comparison (APC) methods [8]. Unfortunately, the antenna positioner used did not allow the displacement of the AUT within the quiet zone to apply these techniques. Nevertheless, the level of the spurious signals is relatively low and the measured pattern does not suffer from many significant extraneous lobes.

2) *Effect of Systematic Quiet-Zone Field Distortions:* Systematic quiet-zone field distortions affect also the main beam region, i.e., the beam width and shape, and not just the sidelobe level. The effect of the systematic distortions is difficult to eliminate from the antenna pattern using APC methods, as these methods are not practically applicable in the main beam region of the pattern.

Imperfect operation of the collimating element produces a nonideal plane wave in the quiet zone of the CATR, which affects the measured beam by distorting the effective aperture field of the antenna. Distortions to the antenna aperture field due to the nonideal quiet-zone field can be determined in the spatial domain at each polarization by multiplying the distortion-free aperture field vector  $\vec{E}_{\text{aperture}}$  by the measured quiet-zone field vector  $\vec{E}_{\text{quietzone}}$

$$\vec{E}_{\text{effective}}(x, y) = \vec{E}_{\text{aperture}}(x, y) \cdot \vec{E}_{\text{quietzone}}(x, y) \quad (1)$$

where  $x$  and  $y$  are the coordinates in the aperture of the antenna.

We use the simulated aperture field of the AUT and the measured cuts of the quiet-zone field to estimate the effect of the quiet-zone field quality on the measurement results. The effective aperture field of the AUT is computed with (1) and the radiation pattern of the AUT is obtained with Fourier transformation from  $\vec{E}_{\text{effective}}(x, y)$ . The two-dimensional field incident on the aperture of the AUT is estimated by interpolating the measured horizontal, vertical, and both diagonal cuts of the quiet-zone field amplitude and phase at the points between the measured cuts, as it was not possible to take a very large number of samples of the quiet-zone field. The relatively few samples in the polar scan of the quiet zone do not allow us to make very accurate predictions of the effect on the antenna pattern over a wide angular range, but a qualitative analysis of the main beam shape distortions can be done. The simulated radiation pattern of the AUT is shown in Fig. 17 and the estimated radiation pattern after taking into account the measured quiet-zone field is shown in Fig. 18. In Fig. 19, the measured, simulated, and estimated  $H$ -plane radiation pattern, which includes the effect of

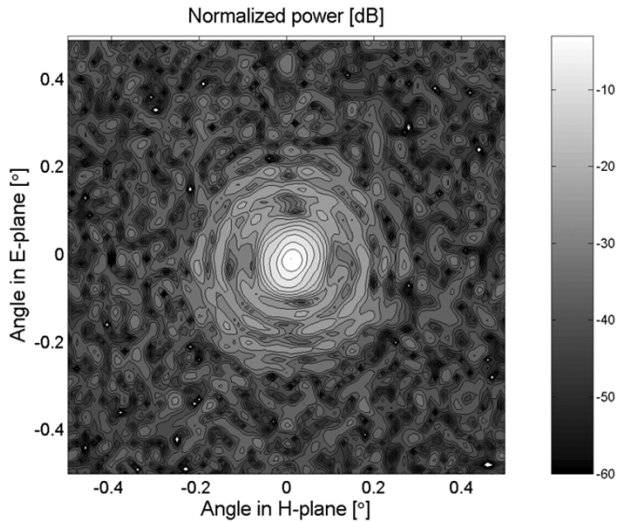


Fig. 17. Contour plot of the simulated radiation pattern at 322 GHz. The contour interval is 3 dB.

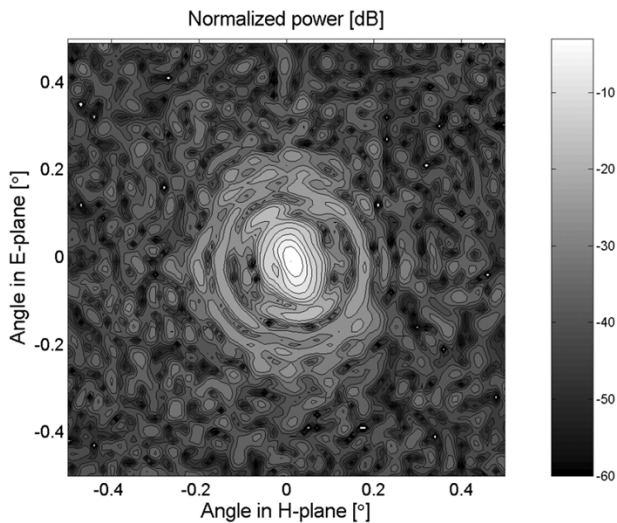


Fig. 18. Contour plot of the estimated radiation pattern at 322 GHz taking into account the effect of the quiet-zone field on the simulated pattern. The contour interval is 3 dB.

the quiet-zone field quality on the simulated radiation pattern, are presented. The E-plane pattern cuts are in Fig. 20.

The nonideal quiet-zone distorts the measured radiation pattern and changes the measured antenna beam shape, as can be seen in Figs. 17 and 18. The contours of the radiation pattern are roughly elliptical in shape near the main beam peak, and the nonideal quiet-zone field distorts the shape of these contours. Quadratic phase errors, i.e., phase front curvature, cause shoulders to the main beam and increase the side-lobe levels [9]. The main beam is also widened. Feed offset causes a nonsymmetrical aperture illumination and antenna pattern [10]. The slight dip in the quiet-zone field amplitude acts opposite to the taper in an antenna aperture field increasing the side-lobe level. However, based on the estimated effect of the quiet-zone field on the simulated antenna pattern, the effect of the quiet-zone field distortions is not large enough to explain alone all the discrepancies between the measurements and simulations. The effect of the deviations in the antenna structure from the designed structure is discussed next.

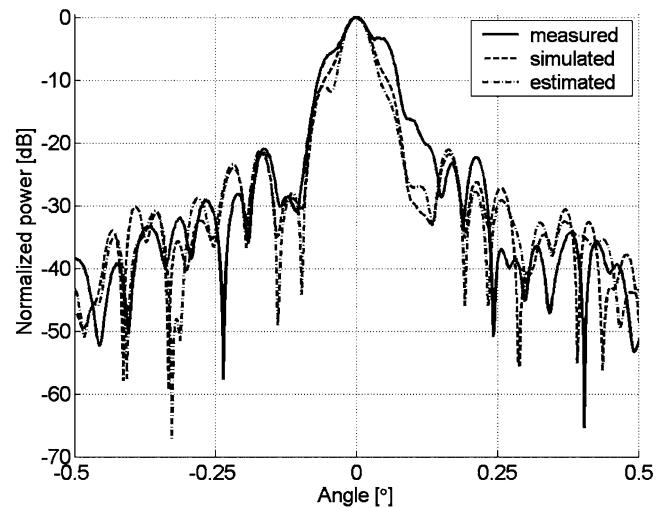


Fig. 19.  $H$ -plane cut showing the measured, simulated, and estimated pattern including effect of the quiet-zone field quality.

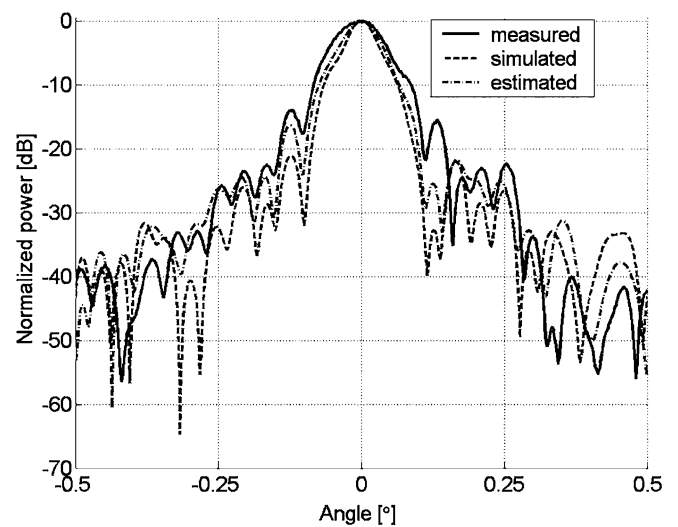


Fig. 20.  $E$ -plane cut showing the measured, simulated, and estimated pattern including effect of the quiet-zone field quality.

### B. Effect of the Deviations in the Structure of the AUT

The AUT consists of a single offset paraboloid fed with a quasi-optical feed located at the paraboloid focus. The surface of the reflector was measured at EADS Astrium with 396 points before the RTO was assembled and the reflector bending was estimated at EADS Astrium. The measured surface distortions from the ideal paraboloid with the estimated reflector bending are shown in Fig. 21. The simulated  $H$ -plane pattern of the distorted paraboloid is compared to the ideal paraboloid in Fig. 22.

The other possible deviations of the antenna structure include feed misalignment and dislocation (offset). Due to the large  $f/D$  ratio, a large feed misalignment is needed to produce clearly visible beam distortions. Such a large misalignment is unlikely to exist in the RTO, as it should be clearly visible. The position of the feed was varied in GRASP8 simulations and the effect on the main beam shape was observed. Fig. 23 shows the measured and the simulated radiation pattern with the estimated effect of the nonideal quiet-zone field when the feed was relocated to  $(+4, 0, -6)$ , in millimeters, in relation to the paraboloid focus at

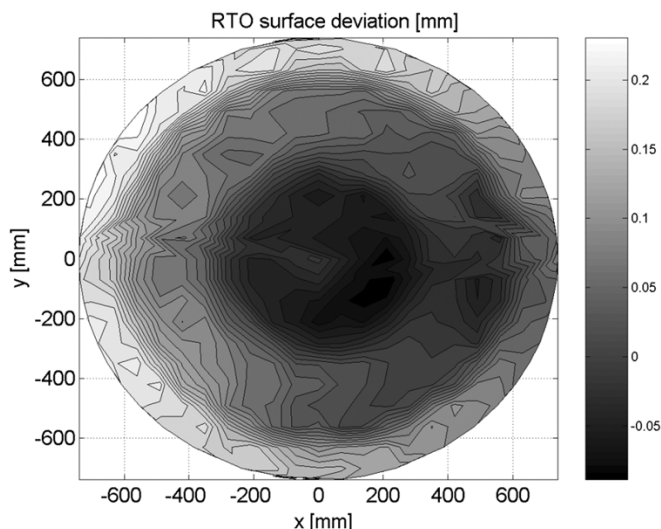


Fig. 21. The surface distortions of the RTO reflector.

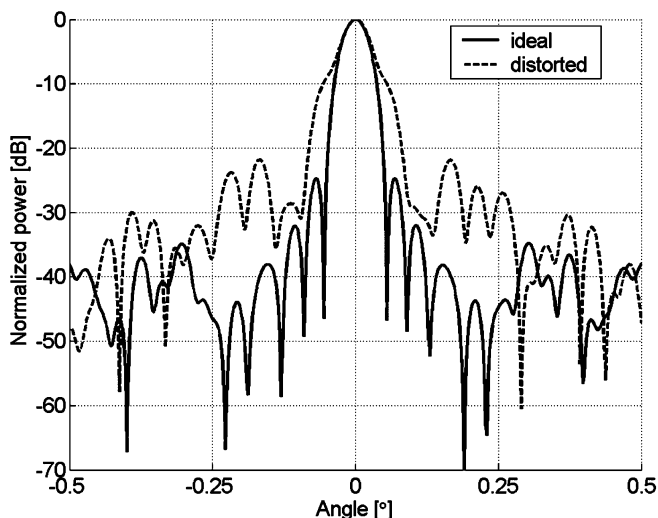


Fig. 22. Simulated  $H$ -plane pattern of the ideal and the distorted paraboloid.

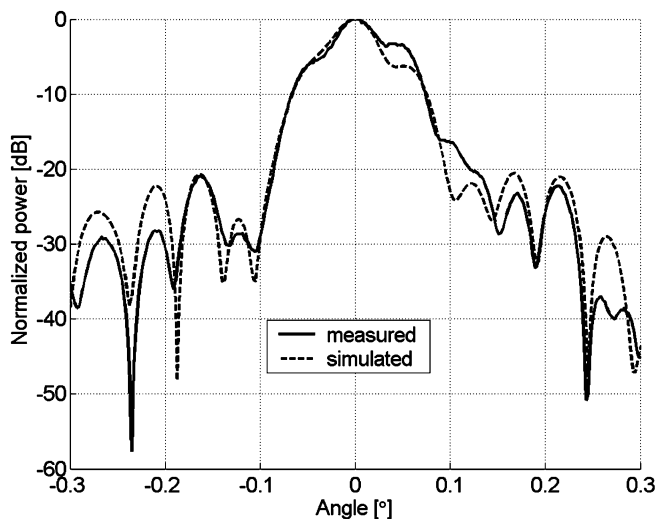


Fig. 23. Simulated radiation pattern with the AUT feed offset including the estimated effect of the quiet-zone field compared to the measured radiation pattern cut in the  $H$ -plane.

(0,0,0) in the  $xyz$  coordinate system, where the  $z$  axis is pointing toward the reflector and the  $x$  axis is the horizontal axis.

This feed offset is quite large and unlikely to be real at this extent. Instead, it is more likely that the phase error in the quiet-zone field and the aperture phase error due to the reflector surface distortions are causing a beam distortion similar to a large feed offset.

## V. DISCUSSION

At submillimeter waves, even relatively small reflector surface errors are large compared to the wavelength, and they have a great effect on the radiation pattern of the antenna as can be seen in Fig. 22. The distorted reflector surface causes the antenna beam to resemble more a contoured beam in a noncontrolled fashion than a pencil beam. In the case of ADMIRALS RTO, the contours of the antenna pattern are approximately elliptical in shape. Measuring only horizontal and vertical cuts of the radiation pattern does not give a full picture on the beam characteristics, and even relatively large beam distortions caused by measurement errors and distortions in the antenna structure are not very easily recognized in the pattern cuts. Therefore, contour maps of the antenna pattern should be measured whenever possible when submillimeter wavelength antennas are tested.

The combined effect of the potential error sources makes the identification of the exact cause for the observed radiation pattern anomalies difficult, and further analysis is needed. However, it seems that the radiation pattern of the AUT, the RTO, deviates from the expected pattern also due to errors in the antenna structure. The accurate analysis of the RTO measurements requires more information on the structure of the antenna with more accurate reflector surface measurements on the operational antenna and with verification of the feed positioning and alignment. Also, to analyze the antenna performance more accurately, the quiet-zone field quality should be better in order to eliminate distortions to the measured antenna pattern due to the nonideal quiet-zone field.

## VI. CONCLUSION

Compact antenna test range based on a hologram was used to test a submillimeter wavelength reflector antenna, ADMIRALS RTO, at a frequency of 322 GHz. The copolar radiation pattern was measured at the vertical polarization, and the cross-polar pattern cuts were measured by changing the AUT receiver polarization to horizontal. The main beam region was measured in two dimensions at the vertical polarization. The estimated dynamic range in the measurements was about 85 dB.

The measurement results were compared to the simulated radiation pattern of the ADMIRALS RTO. The measured results correspond reasonably well with the simulated pattern. The shape of the reflector surface was included in the simulation of the antenna radiation. The measured  $-3$  dB beam width is  $0.086^\circ$  in the  $E$ -plane and  $0.050^\circ$  in the  $H$ -plane. The simulated beam widths are  $0.053^\circ$  and  $0.045^\circ$ .

The effect of the nonideal quiet-zone field on the measurement results was investigated by computing the radiation of the simulated antenna including the effect of the measured quiet-zone field. The quiet-zone field amplitude and phase in the antenna aperture were estimated from the measured horizontal, vertical,

and diagonal cuts, and radiation pattern was then computed by including the quiet-zone field distortions into the aperture field. The quiet-zone field has significant effect on the measurement results. An extraneous lobe around the direction of  $-8^\circ$  in the H-plane (horizontal) cut of the antenna pattern was identified to be caused by an external scatterer in the measurement hall. Also the structure of the antenna under test, especially the reflector surface shape, has a great effect on the radiation pattern. Therefore, in general at submillimeter wavelengths, measured contour maps of the antenna pattern should be used in the analysis of the antenna performance, as using only the horizontal and vertical pattern cuts does not give a full picture on the shape of the antenna beam. Further information on the structure of ADMIRALS RTO and/or more antenna pattern measurements are needed for more accurate antenna performance analysis.

The antenna tests described in this paper were the first that were done using a CATR based on a hologram at submillimeter wavelengths. The test results of the ADMIRALS RTO at 322 GHz show great promise for the hologram-based CATR at submillimeter wavelengths. Future research will focus on improving the quiet-zone field quality and on increasing the quiet-zone size, allowing tests of larger antennas at shorter submillimeter wavelengths.

#### ACKNOWLEDGMENT

E. Kahra, S. Ranvier, H. Rönnerberg, and L. Laakso are thanked for their valuable assistance in the construction of the CATR and its instrumentation. J. Lemanczyk from ESA/ESTEC is acknowledged for his advice and support in the hologram CATR development. Dr. J. Hartmann from EADS Astrium is acknowledged for the ADMIRALS RTO reflector surface data. VTT Information Technology and CSC (Finnish IT Center for Science) are acknowledged for providing software and computer resources.

#### REFERENCES

- [1] T. Hirvonen, J. Ala-Laurinaho, J. Tuovinen, and A. V. Räsänen, "A compact antenna test range based on a hologram," *IEEE Trans. Antennas Propag.*, vol. 45, pp. 1270–1276, 1997.
- [2] A. Lönnqvist, T. Koskinen, J. Häkli, J. Säily, J. Ala-Laurinaho, J. Mallat, V. Viikari, J. Tuovinen, and A. V. Räsänen, "Hologram-based compact range for submillimeter wave antenna testing," *IEEE Trans. Antennas Propag.*, to be published.
- [3] J. Ala-Laurinaho, T. Hirvonen, P. Piironen, A. Lehto, J. Tuovinen, A. V. Räsänen, and U. Frisk, "Measurement of the Odin telescope at 119 GHz with a hologram-type CATR," *IEEE Trans. Antennas Propag.*, vol. 49, pp. 1264–1270, 2001.
- [4] J. Häkli, J. Ala-Laurinaho, T. Koskinen, J. Lemanczyk, A. Lönnqvist, J. Mallat, A. V. Räsänen, J. Säily, J. Tuovinen, and V. Viikari, "Sub-mm antenna tests in a hologram CATR," in *Proc. 26th AMTA Symp.*, Atlanta, GA, 2004, pp. 238–242.
- [5] J. Hartmann, J. Habersack, H.-J. Steiner, T. Rose, and P. Zimmermann, "Transmit and receive modules for measurement of future space applications in the terahertz region," in *Proc. 23rd AMTA Symp.*, Denver, CO, 2001, pp. 171–176.
- [6] J. Hartmann, J. Habersack, H.-J. Steiner, J. Lemanczyk, and P. de Maagt, "Calibration and verification measurements in compensated compact ranges up to 500 GHz," in *Proc. 23rd AMTA Symp.*, Denver, CO, 2001, pp. 377–382.
- [7] J. Ala-Laurinaho, T. Sehm, J. Säily, and A. V. Räsänen, "Cross-polarization performance of the hologram compact antenna test range,"  *Microwave Opt. Technol. Lett.*, vol. 27, no. 4, pp. 225–229, 2000.
- [8] J. Appel-Hansen, "Reflectivity level of radio anechoic chambers," *IEEE Trans. Antennas Propag.*, vol. AP-21, pp. 490–498, 1973.
- [9] P. S. Hacker and H. E. Schrank, "Range distance requirements for measuring low and ultralow sidelobe antenna patterns," *IEEE Trans. Antennas Propag.*, vol. AP-30, pp. 956–966, 1982.
- [10] G. E. Evans, *Antenna Measurement Techniques*. Boston, MA: Artech House, 1990, pp. 229–229.



**Janne Häkli** (S'97–M'05) was born in Helsinki, Finland, in 1972. He received the Master of Science (Tech.) and Licentiate of Science (Tech.) degrees in electrical engineering from Helsinki University of Technology (TKK), Espoo, Finland, in 1999 and 2002, respectively, where he is currently pursuing the Doctor of Science (Tech.) degree.

Since 1998, he has been a Research Assistant and Research Engineer with the Radio Laboratory, TKK. His current research interests include submillimeter-wave shaped reflector antennas, antenna measurement techniques, and hologram applications.



**Tomi Koskinen** (S'03) was born in Jämsä, Finland, in 1975. He received the Master of Science (Tech.) and Licentiate of Science (Tech.) degrees in electrical engineering from Helsinki University of Technology (TKK), Espoo, Finland, in 2001 and 2004, respectively, where he is currently pursuing the Doctor of Science (Tech.) degree.

Since 2001, he has been a Research Engineer with the Radio Laboratory, TKK. His fields of interest are radio engineering and electromagnetics, especially computational electromagnetics. He is currently developing a hologram-based CATR for very large submillimeter-wave antennas.



**Anne Lönnqvist** was born in Somero, Finland, in 1977. She received the Master of Science (Tech.) (with honors) and Licentiate of Science (Tech.) degrees in electrical engineering from Helsinki University of Technology (TKK), Espoo, Finland, in 2001 and 2004, respectively, where she is currently pursuing the Doctor of Science (Tech.) degree.

Since 2000, she has been a Research Assistant and a Research Engineer with the Radio Laboratory, TKK. Her current research interests include millimeter-wave measurement techniques with a focus

on hologram applications.



**Jussi Säily** was born in Rantsila, Finland, in 1974. He received the Master of Science (Tech.), Licentiate of Science (Tech.), and Doctor of Science (Tech.) degrees in electrical engineering from Helsinki University of Technology (TKK), Espoo, Finland, in 1997, 2000, and 2003, respectively.

In 1996, he was a Research Trainee with the VTT Technical Research Centre, Finland Automation/Measurement Technology Laboratory, where he studied microelectromechanical sensors. From 1997 to 2003, he was a Research Engineer with the Radio Laboratory, TKK. Since 2004, he has been with the Antennas and Electromagnetics research group, VTT Technical Research Centre. His current research interests include beam-steerable millimeter-wave antenna arrays for short-range communications, smart base-station antenna arrays for telecommunications, and low-noise signal sources for instrumentation.



**Ville Viikari** (S'04) was born in Espoo, Finland, in 1979. He received the Master of Science (Tech.) degree in electrical engineering from Helsinki University of Technology (TKK), Espoo, Finland, in 2004, where he is currently working toward the Doctor of Science (Tech.) degree.

Since 2001, he has been a Trainee, Research Assistant, and Research Engineer with the Radio Laboratory (TKK). His current research interest is the development of the antenna measurement techniques at submillimeter wavelengths.



**Juha Mallat** was born in Lahti, Finland, in 1962. He received the Master of Science (Tech.) (with honors), Licentiate of Science (Tech.), and Doctor of Science (Tech.) degrees in electrical engineering from Helsinki University of Technology (TKK), Espoo, Finland, in 1986, 1988, and 1995, respectively.

Since 1985, he has been with the Radio Laboratory (and its Millimeter Wave Group), TKK, as a Research Assistant, Senior Teaching Assistant, and Research Associate until 1994. From 1995 to 1996, he was a Project Manager and Coordinator in an education project between TKK and the Turku Institute of Technology.

Since 1997, he has been a Senior Scientist with the Millimeter Wave Laboratory of Finland (MilliLab), European Space Agency (ESA) External Laboratory, with the exception of one year during 2001–2002, when he was a Professor (protem) of radio engineering with TKK. His research interests and experience cover various topics in radio-engineering applications and measurements, especially in millimeter-wave frequencies. He has also been involved in building and testing millimeter-wave receivers for space applications.



**Juha Ala-Laurinaho** was born in Parkano, Finland, on July 4, 1969. He received the Master of Science (Tech.) degree in mathematics and the Licentiate of Science (Tech.) and Doctor of Science (Tech.) degrees in electrical engineering from Helsinki University of Technology (TKK), Espoo, Finland, in 1995, 1998, and 2001, respectively.

Since 1995, he has been a Research Assistant and Research Engineer with the Radio Laboratory, TKK. His current research interest is the development of antenna measurement techniques for millimeter and

submillimeter waves.



**Jussi Tuovinen** (S'86–M'91) received the Dipl. Eng., Lic. Tech., and Dr. Tech. degrees in electrical engineering from Helsinki University of Technology (TKK), Espoo, Finland, in 1986, 1989, and 1991, respectively.

During 1986–1991, he worked as a Research Engineer with TKK Radio Laboratory, where he was involved with millimeter-wave antenna testing for European Space Agency (ESA), quasi-optical measurements, and Gaussian-beam theory. From 1991 to 1994, he was with the Five College Radio

Astronomy Observatory, University of Massachusetts, Amherst, as a Senior Postdoc, where he studied holographic test methods for large telescopes and developed frequency multipliers up to 1 THz. From 1994 to 1995, he was a Project Manager with TKK Radio Laboratory, involved with hologram CATR and 119-GHz receiver development for the Odin-satellite. From 1995 to 2004, he was the Director of the Millimeter Wave Laboratory of Finland—MilliLab, ESA External Laboratory. He is a coinvestigator and heads the development of 70-GHz receivers for the Low Frequency Instrument of the ESA Planck Mission. His research activities also include development of methods for on-wafer testing of integrated circuits and components, as well as imaging systems and MEMS at millimeter wave. Since 1999, he has been a Research Professor with VTT Information Technology, Espoo. During 2001–2002, he worked as a Visiting Researcher at the University of Hawaii at Manoa, where he developed multipath communications methods using retrodirective antennas. In 2004, he was appointed Research Director of VTT Information Technology. He has authored or coauthored more than 150 scientific papers.

Dr. Tuovinen received ESA Fellowships for multiplier work at the University of Massachusetts in 1992 and again in 1993. He is a past secretary of the Finnish National Committee of the Committee on Space Research (COSPAR) and the IEEE Finland Section. He was also the Executive Secretary of the Local Organizing Committee of the 27th Plenary Meeting of COSPAR held in 1988. In 1998, he was the Co-Chairman of the 2nd ESA Workshop on Millimeter Wave Technology and Applications. He has also served as a Chairman of the IEEE MTT/AP Finland Chapter. In 2003, he served as the Chairman of the 3rd ESA Workshop on Millimeter Wave Technology and Applications.



**Antti V. Räsänen** (S'76–M'81–SM'85–F'94) received the Diploma Engineer (M.Sc.), Licentiate of Science (Tech), and Doctor of Science (Tech) degrees in electrical engineering from the Helsinki University of Technology (TKK), Espoo, Finland, in 1973, 1976, and 1981, respectively.

In 1989, he was appointed Professor Chair of Radio Engineering, TKK, after holding the same position as an Acting Professor in 1985 and 1987–1989. In 1997, he became Vice-Rector of TKK for 1997–2000. He has been a Visiting Scientist and

Professor with the Five College Radio Astronomy Observatory (FCRAO) and the University of Massachusetts, Amherst (1978–1981), Chalmers University of Technology, Göteborg, Sweden (1983), Department of Physics, University of California at Berkeley (1984–1985), Jet Propulsion Laboratory, California Institute of Technology, Pasadena (1992–1993), and Paris Observatory and University of Paris 6 (2001–2002). He currently supervises research in millimeter-wave components, antennas, receivers, microwave measurements, etc., at the Radio Laboratory, TKK, and Millimeter Wave Laboratory of Finland (MilliLab—European Space Agency (ESA) External Laboratory). The Smart and Novel Radios Research Unit (SMARAD), TKK (which he leads), received the national status of Center of Excellence in Research from The Academy of Finland in 2001 after competition and international review. He has authored and coauthored about 400 scientific or technical papers and six books, most recently *Radio Engineering for Wireless Communication and Sensor Applications* (MA: Artech House, 2003). He also coauthored the chapter “Radio-Telescope Receivers” in *Radio Astronomy* by J. D. Kraus (Powell, OH: Cygnus-Quasar, 1986, 2nd edition).

Dr. Räsänen was the Chairman of the IEEE MTT/AP Chapter in Finland from 1987 to 1992. He was the Secretary General of the 12th European Microwave Conference in 1982, and served as the Conference Chair for the 22nd European Microwave Conference in 1992, and Chair and Co-Chair for the 2nd ESA Workshop on Millimeter Wave Technology and Applications: antennas, circuits, and systems in 1998, and the 3rd ESA Workshop on Millimeter Wave Technology and Applications: circuits, systems, and measurement techniques in 2003, respectively. He is Conference Chairman of the International Joint Conference of the 4th ESA Workshop on Millimeter-Wave Technology and Applications, the 8th Topical Symposium on Millimeter Waves TSMMW2006, and the 7th MINT Millimeter-Wave International Symposium MINT-MIS2006 in 2006. During 1995–1997 he served in the Research Council for Natural Sciences and Engineering, the Academy of Finland. From 2002 to 2005 he served as an Associate Editor of the IEEE TRANSACTIONS ON MICROWAVE THEORY AND TECHNIQUES.